



## A Spectrophotometric Study of the Acid–Base Equilibria of *o*-Methyl Red in Aqueous Solutions

Khalid M. Tawarah & Hakam M. Abu-Shamleh

Department of Chemistry, Yarmouk University, Irbid, Jordan

(Received 12 March 1991; accepted 22 April 1991)

### ABSTRACT

*The UV–visible spectra of o-methyl red were examined at 25°C in water at various acidities and the variations in the spectra were correlated with the structures of the several forms of the compound. The two acid–base equilibria that involve the monoprotonated form of o-methyl red were treated as overlapping equilibria. The thermodynamic acid dissociation constants ( $K_{a2}$  and  $K_{a3}$ ) of the diprotonated and the monoprotonated forms were found to be  $(4.16 \pm 0.14) \times 10^{-3}$  and  $(1.40 \pm 0.02) \times 10^{-5} \text{ mol dm}^{-3}$ , respectively. Complete extraction of o-methyl red from the aqueous phase into the  $\text{CCl}_4$  phase was observed in the pH range 1.25–5.6. The significance of this result with respect to the structure of the monoprotonated form is discussed.*

### 1 INTRODUCTION

Several authors have suggested the use of *o*-methyl red, *o*-(*p*-dimethylaminophenylazo)benzoic acid, as an example for determining the  $\text{p}K$  value of an acid–base indicator by a spectrophotometric method.<sup>1–4</sup> The suggestion is based on a general indicator equilibrium, given as  $\text{HIn} \rightleftharpoons \text{H}^+ + \text{In}^-$ , where HIn,  $\text{In}^-$  and  $K$  are the acid form, the alkaline form and the acid dissociation constant of the indicator, respectively. The use of *o*-methyl red as an indicator for acid–base titrations in aqueous solutions is based on the observation that the indicator changes its colour in the pH range 4.2–6.3.<sup>2</sup>

Two questions can be raised concerning the applicability of the above equilibrium to the case of *o*-methyl red. The first is concerned with the

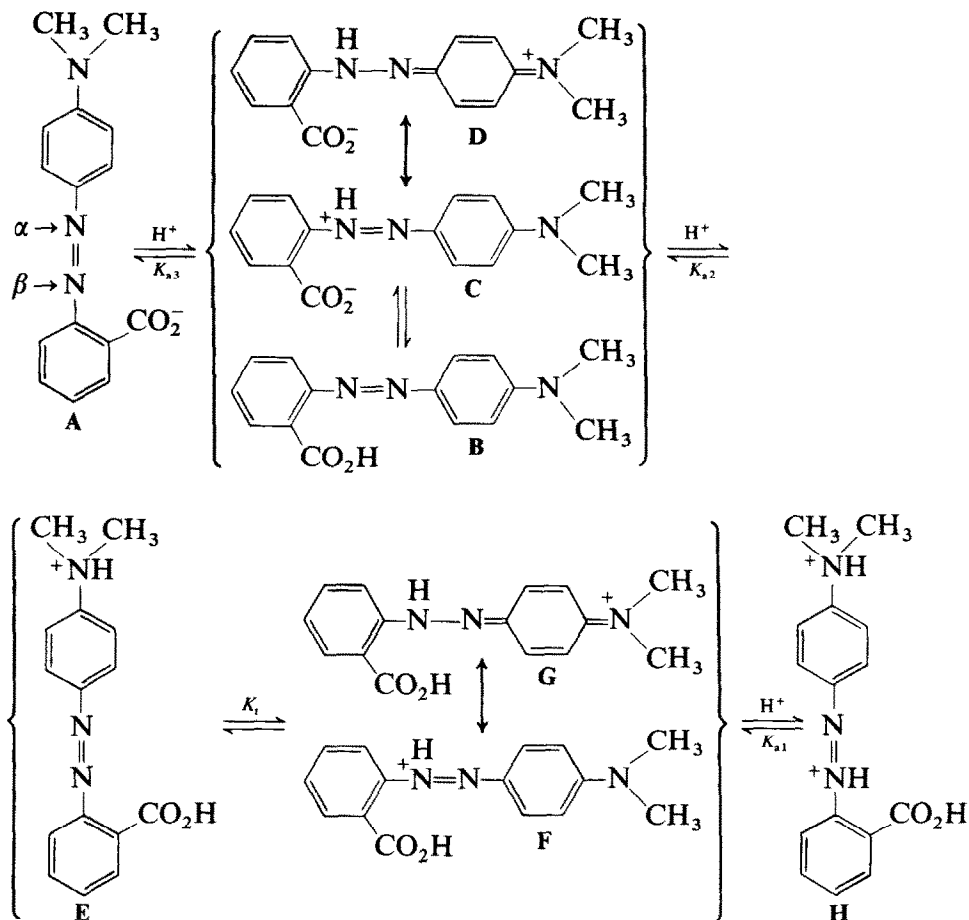


Fig. 1. The acid-base equilibria of *o*-methyl red in aqueous acidic solutions.

structure of the monoprotonated species,  $\text{HIn}$ , in aqueous solutions. It has been assumed that the monoprotonated form is a resonance hybrid of a zwitterion<sup>1-3</sup> (structures **C** and **D**, Fig. 1). However, Williams<sup>5</sup> has suggested a nonionic structure, where the first proton adds to the carboxyl anion (structure **B**, Fig. 1). The nonionic structure can thus give resonating zwitterionic structures, in which the  $\beta$ -nitrogen of the azo linkage forms a six-membered ring with the  $-\text{COOH}$  group, via hydrogen bonding. The presence of such resonating structures was considered<sup>5</sup> as an explanation for *o*-methyl red changing colour from yellow to red at the first protonation at pH 4.9, while *p*-methyl red changed colour at the second protonation at pH 2.1. *o*-Methyl red is therefore assumed to have two red forms, one form being associated with the monoprotonated form at pH 4.9 and the second with the diprotic form at pH 2.1.

The second question is concerned with the validity of the assumption that, at some pH value, *o*-methyl red is completely present in the monoprotonated form.<sup>1-4</sup> In order to evaluate this problem, it is necessary to appreciate that *o*-methyl red has four possible basic centres to which a proton can be added. These centres are the  $\text{—COO}^-$  group, the  $\alpha$ - and  $\beta$ -nitrogens of the azo linkage, and the nitrogen of the dimethylamino group. Literature data<sup>5</sup> concerning the values of the acid dissociation constants ( $K_{a2}$  and  $K_{a3}$ , Fig. 1) corresponding to equilibria involving the monoprotonated form indicates that the two equilibria are overlapping. This means that *o*-methyl red cannot be present solely in the monoprotonated form in aqueous solutions. Therefore, the suggestion<sup>1-4</sup> of determining the  $pK$  value of *o*-methyl red ( $pK_{a3}$ , Fig. 1) by a spectrophotometric method is an oversimplification. Ramette *et al.*<sup>6</sup> concluded that  $K_{a2}$  and  $K_{a3}$  describe two overlapping equilibria and suggested a computational method that involves parameter adjustment for determining  $K_{a2}$  and  $K_{a3}$  from the visible spectra of *o*-methyl red.

The purpose of the present work is to examine the UV-visible spectrum of *o*-methyl red in aqueous solutions of varying acidity and to establish values for  $K_{a2}$  and  $K_{a3}$  at 25°C in a manner somewhat different from that of Ramette *et al.*<sup>6</sup> In order to clarify the structure of the monoprotonated form of *o*-methyl red, a qualitative study concerning the distribution of *o*-methyl red between  $\text{CCl}_4$  and the aqueous phase is also attempted. The structures proposed in Fig. 1 are to be considered as the conceivable structures of *o*-methyl red in water, and can be compared with structures proposed for other aminoazobenzene dyes.<sup>7-9</sup> The protonation of the  $\alpha$ -nitrogen of the azo linkage was ignored on the basis of the argument given by Yeh and Jaffe.<sup>10</sup>

## 2 EXPERIMENTAL

The acid form of *o*-methyl red ( $\text{C}_{15}\text{H}_{15}\text{N}_3\text{O}_2$ ) was purchased from Sigma and was recrystallized from methanol. The test sample was dried at 90°C for 16 h before use. Distilled, deionized and freshly boiled water was used for preparing a stock solution of *o*-methyl red, and no alcohol was used in such preparations. A carbonate-free aqueous NaOH solution was used to enhance the solubility of *o*-methyl red in water. A typical stock solution of *o*-methyl red had a concentration of  $1.86 \times 10^{-4} \text{ mol dm}^{-3}$ , an ionic strength of  $2.2 \times 10^{-3} \text{ mol dm}^{-3}$  and a pH value of 11. Under these conditions the *o*-methyl red is present as the sodium salt. The molar absorptivities at 430 and 520 nm, as well as the pH of the stock solution, were found to be constant over a storage period of several months.

The pH of a test solution was adjusted by adding an appropriate amount of either HCl or NaOH solution. In the distribution experiments, equal

volumes (20 cm<sup>3</sup> each) of CCl<sub>4</sub> and an aqueous solution of *o*-methyl red were used. After the attainment of equilibrium at ambient temperature (about 18°C), the colour of each phase was noted.

The UV-visible spectra were recorded at 25.0 ± 0.1°C, using a double-beam spectrophotometer (DMS 100, Varian) equipped with a thermostated cell holder. Stoppered quartz cells with an optical path length of 1.00 cm were used. The pH measurements were carried out using an Orion Research Digital Ionizer equipped with a combined pH electrode (Orion, research grade electrode). The meter was calibrated by using phthalate, phosphate and borax buffer solutions as suggested by Albert and Serjeant.<sup>11</sup>

### 3 RESULTS AND DISCUSSION

Figure 2 shows the UV-visible spectrum of *o*-methyl red in the pH range 0.5–10. The presence of more than one isosbestic point in the figure is an indication of the presence of more than one acid–base equilibrium. The UV absorption at  $\lambda_{\text{max}} = 290$  nm is probably an  $n \rightarrow \pi^*$  transition due to the —COO<sup>−</sup> or —COOH group, because we have found that methyl orange

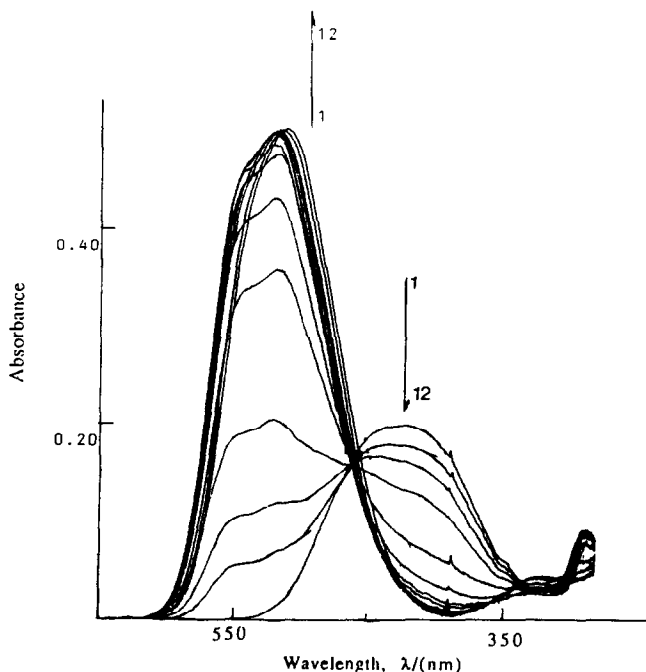


**Fig. 2.** The UV-visible spectrum of  $9.24 \times 10^{-6}$  mol dm<sup>−3</sup> *o*-methyl red as a function of pH. Curves 1–12 correspond to the pH values 10.0, 6.01, 5.69, 5.36, 4.77, 3.87, 3.62, 3.07, 2.78, 2.35, 1.84 and 0.50, respectively.

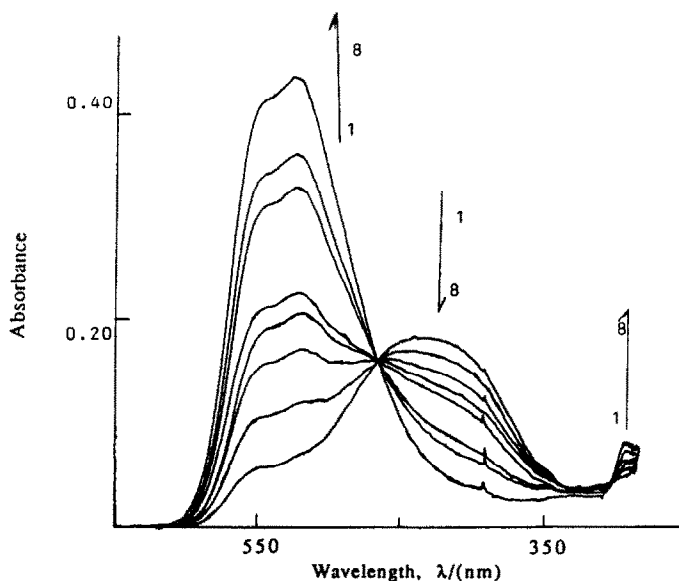
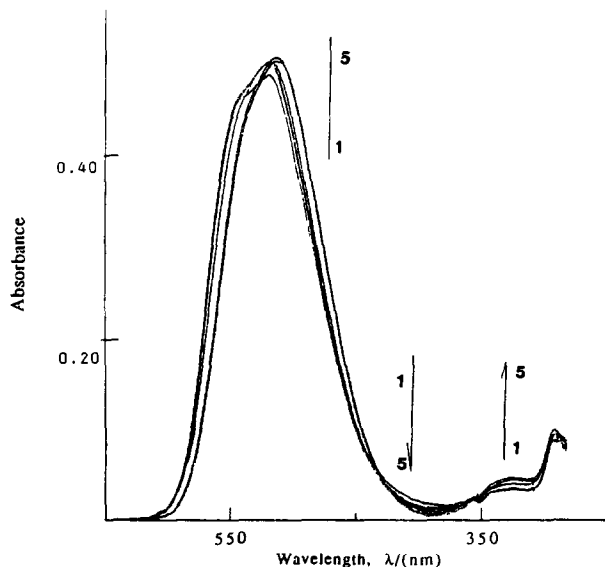


Fig. 3. The UV-visible spectrum of  $9.24 \times 10^{-6} \text{ mol dm}^{-3}$  *o*-methyl red as a function of pH. Curves 1–8 correspond to the pH values 6.01, 5.69, 5.58, 5.36, 5.30, 4.92, 4.77 and 3.87, respectively.

and methyl yellow do not give rise to such an absorption, while *p*-methyl red shows such an absorption. The broad maximum centred at about 430 nm is due to the yellow anion form of *o*-methyl red and the intense absorption at about 520 nm is due to the red protonated form.

For clarification, the spectra of Fig. 2 were subdivided into two sets. The first set is shown in Fig. 3, which covers the pH range 3.87–6.01. It is evident from this figure that, as the pH is lowered, the intensity of the band centred at 430 nm decreases and a new band centred at about 525 nm starts to develop, indicating the presence of the red acidic form. This absorption is attributed to the monoprotinated form, which is assumed to be a mixture of a nonionic structure and a resonance hybrid of the zwitterionic structures **B**, **C** and **D** (Fig. 1). The isosbestic point at 466 nm represents the first macroscopic protonation equilibrium with an acid dissociation constant  $K_{a3}$ . Spectra having this isosbestic point were used in this study for calculating  $K_{a3}$ .

The second set of spectra is shown in Fig. 4, which covers the pH range 0.5–3.1. It is evident that the lowering of pH is accompanied by a blue shift in the absorption maximum of the red-coloured species, from 525 to 518 nm. The absorption maximum at 518 nm is attributed to a diprotinated form. A weak broad band develops at about 325 nm, and becomes appreciable as the pH is lowered. The intensity of the absorption at 290 nm is almost constant with respect to variations in pH, indicating that the carboxyl anion is fully



**Fig. 4.** The UV-visible spectrum of  $9.24 \times 10^{-6} \text{ mol dm}^{-3}$  *o*-methyl red as a function of pH. Curves 1–5 correspond to the pH values 3.07, 2.78, 2.35, 1.84 and 0.50, respectively.

protonated. Based on literature information<sup>7–9</sup> on the spectra of substituted azobenzene dyes, the absorption maximum at 518 nm is attributed to the azonium tautomer (resonance hybrid of structures G and F, Fig. 1) while the weak absorption at 325 nm is attributed to the ammonium tautomer (structure E, Fig. 1). The ratio of the absorbances at 518 and 325 nm at pH 0.5 (spectrum 5, Fig. 4) is 11. Such a high ratio has been reported for *o*-methyl red in  $1.2 \text{ mol dm}^{-3}$  HCl in aqueous ethanol.<sup>9</sup> Spectra recorded in the pH range  $0.5 < \text{pH} < 3$  were used in this study for calculating  $K_{a2}$ .

The UV-visible spectrum of *o*-methyl red was not affected by changes in the HCl concentration within the range  $0.1\text{--}1 \text{ mol dm}^{-3}$ . This was indicated by the constancy in the absorbance values at 518, 325 and 290 nm. This observation is considered as evidence for *o*-methyl red being in the diprotonated form. Further increase in the concentration of HCl, up to  $7 \text{ mol dm}^{-3}$ , resulted in small changes in the intensities of the tautomer bands at 518 and 325 nm, the absorption at 518 nm slightly increasing and that at 325 nm slightly decreasing. However, these changes in the intensities of the *o*-methyl red tautomers amount to about 10% of their counterparts in methyl orange or methyl yellow.<sup>12</sup> This difference indicates that the tautomeric equilibrium of *o*-methyl red (equilibrium designated by  $K_t$  in Fig. 1) is less sensitive to changes in the HCl concentration compared with that of methyl orange or methyl yellow.

**TABLE 1**  
Effects of pH and HCl Concentration on the Distribution  
of *o*-Methyl Red between CCl<sub>4</sub> and H<sub>2</sub>O at About 18°C

<i>pH</i> or [HCl]	CCl <sub>4</sub> extraction	Colour in H <sub>2</sub> O layer
> 7	Nil	Yellow
6-7	Trace	Yellow
5.7-6.0	Appreciable	Light yellow
1.25-5.6	Complete	Colourless
0.46M	Minor	Red
1.0M	Trace	Red
2-5M	Nil	Red

A possible explanation for the behaviour of *o*-methyl red can be given with reference to the tautomeric equilibrium given in Fig. 1. It appears that the presence of the —COOH group in *o*-methyl red stabilizes the azonium tautomer of the diprotic form by forming a six-membered ring via an intramolecular hydrogen bond involving the protonated  $\beta$ -nitrogen of the azo linkage and the carbonyl oxygen of the —COOH group. The formation of such a six-membered ring is also possible in the case of the ammonium tautomer, where the unprotonated  $\beta$ -nitrogen of the azo linkage and the —OH of the —COOH group are intramolecularly hydrogen bonded. Therefore, the engagement of the  $\beta$ -nitrogen of both tautomers in such six-membered structures causes the tautomeric equilibrium of *o*-methyl red to be less sensitive to variations in HCl concentration compared to methyl orange or methyl yellow.

The effect of H<sub>2</sub>SO<sub>4</sub> on the UV-visible spectrum of *o*-methyl red was also investigated. It was observed that, as the concentration of H<sub>2</sub>SO<sub>4</sub> increased, the intensity of the absorption at 518 nm decreased, and a new band centred at 418 nm developed. The colour of the solution became yellow in the presence of 88% (w/w) H<sub>2</sub>SO<sub>4</sub>. This yellow colour is attributed to the formation of the triprotonated form (structure **H**, Fig. 1). No attempt was made in this present study to evaluate  $K_{a1}$  of the triprotonated form. These results indicate that the four macroscopic forms of *o*-methyl red can be associated with the following colours and  $\lambda_{\max}$  values: the triprotonated form is yellow with  $\lambda_{\max} = 418$  nm, the diprotic form is red with  $\lambda_{\max} = 518$  nm, the monoprotic form is red with  $\lambda_{\max} = 525$  nm, and the anion form is yellow with  $\lambda_{\max} = 430$  nm.

The results of the distribution study at about 18°C are summarized in Table 1, which shows the distribution of *o*-methyl red between CCl<sub>4</sub> and the aqueous phase whose pH or HCl concentration is changing. The data in

Table 1 indicate that *o*-methyl red can be quantitatively extracted into  $\text{CCl}_4$  when the pH of the aqueous phase is in the range 1.25–5.6. When the pH is higher than 5.6, or when the HCl concentration is higher than  $0.4 \text{ mol dm}^{-3}$ , the extractability of *o*-methyl red is progressively diminished and becomes nil for pH values  $> 7$  or HCl concentrations  $> 2 \text{ mol dm}^{-3}$ . These results are in agreement with the work of Williams,<sup>13</sup> who used di-*n*-butyl ether instead of  $\text{CCl}_4$ .

The significance of the data in Table 1 to the structures proposed in Fig. 1 is as follows. At pH values  $> 7$ , *o*-methyl red seems to exist entirely in the anion form, which is not extractable. We found that the anion form does not aggregate in the aqueous phase since Beer's law was obeyed at 390, 400, 415, 430, 445, 460 and 480 nm for *o*-methyl red concentrations in the range  $1.86 \times 10^{-6}$ – $1.67 \times 10^{-4} \text{ mol dm}^{-3}$ . However, the unextractability of *o*-methyl red when the concentration of HCl was higher than  $2 \text{ mol dm}^{-3}$  is due to its presence in the positively charged diprotonated form. We have shown in a previous study<sup>14</sup> that the first conjugate acid of methyl yellow (a positively charged species) and the first conjugate acid of methyl orange (a zwitterion) were not extractable into  $\text{CCl}_4$  for HCl concentrations  $> 2 \text{ mol dm}^{-3}$ . Therefore, the extractability of *o*-methyl red at the acidities given in Table 1 seems to be due to the presence of the nonionic structure, and not to the zwitterionic structures of the monoprotonated form.

The recognition of the nonionic structure seems vital in order to explain the results in Table 1. Williams<sup>13</sup> speculated that the colour of the nonionic structure of *o*-methyl red should be yellow in water, since the colour of the organic phase was yellow in a distribution experiment. However, the possibility of having zwitterionic structures in water in addition to the nonionic structure, results in *o*-methyl red appearing red in the aqueous phase.

The determination of the thermodynamic acid dissociation constants  $K_{a2}$  and  $K_{a3}$  of the diprotonated and the monoprotonated forms of *o*-methyl red was based on the following equations:



$$K_{a2} = \frac{[\text{H}^+][\text{HMR}]}{[\text{H}_2\text{MR}^+]} \left( \frac{f_{\text{HMR}} \cdot f_{\text{H}^+}}{f_{\text{H}_2\text{MR}^+}} \right) \quad (2)$$



$$K_{a3} = \frac{[\text{H}^+][\text{MR}^-]}{[\text{HMR}]} \left( \frac{f_{\text{MR}^-} \cdot f_{\text{H}^+}}{f_{\text{HMR}}} \right) \quad (4)$$



where  $\text{H}_2\text{MR}^+$ ,  $\text{HMR}$  and  $\text{MR}^-$  represent the diprotic form, the monoprotic form and the anion form of *o*-methyl red, respectively, and  $f_i$  represents the molar activity coefficient of the designated species. The product,  $[\text{H}^+] \cdot f_{\text{H}^+}$ , which is the activity of the  $\text{H}^+$  ( $a_{\text{H}^+}$ ), was calculated from the pH value of the test solution ( $a_{\text{H}^+} = 10^{-\text{pH}}$ ). The activity coefficient of the neutral form ( $f_{\text{HMR}}$ ) was assumed to be unity. The activity coefficient of the diprotic form ( $f_{\text{H}_2\text{MR}^+}$ ) was calculated according to eqn (5):

$$\log f_{\text{H}_2\text{MR}^+} = -(0.512\sqrt{I}/1 + \sqrt{I}) + 0.20I \quad (5)$$

Equation (5) is the Guggenheim extension of the Debye-Huckel equation for singly charged organic ions<sup>15</sup> in water at 25°C. The symbol  $I$  represents the ionic strength of the solution. The activity coefficient of the anion ( $f_{\text{MR}^-}$ ) was calculated at low ionic strength from the Debye-Huckel limiting law ( $\log f_{\text{MR}^-} = -0.509\sqrt{I}$  in water at 25°C).

Ramette *et al.*<sup>6</sup> have considered the equilibria of eqns (1) and (3) as overlapping equilibria, since the ratio  $[\text{H}^+][\text{HMR}]/[\text{H}_2\text{MR}^+]$ :  $[\text{H}^+][\text{MR}^-]/[\text{HMR}]$  is about 250. We have also assumed that these equilibria are overlapping. In terms of absorbances, eqn (2) can be rewritten in the form

$$K_{a2} = \left( \frac{A - A_a}{A_b - A} \right) \left( \frac{a_{\text{H}^+} \cdot f_{\text{HMR}}}{f_{\text{H}_2\text{MR}^+}} \right) \quad (6)$$

where  $A$ ,  $A_a$  and  $A_b$  represent the absorbances of isomolar solutions of a mixture of  $\text{H}_2\text{MR}^+$  and  $\text{HMR}$ , a solution of  $\text{H}_2\text{MR}^+$  and a solution of  $\text{HMR}$ , respectively. Likewise, eqn (4) can be rewritten in terms of absorbances as follows:

$$K_{a3} = \left( \frac{A' - A'_a}{A'_b - A'} \right) \left( \frac{a_{\text{H}^+} \cdot f_{\text{MR}^-}}{f_{\text{HMR}}} \right) \quad (7)$$

where  $A'$ ,  $A'_a$  and  $A'_b$  are the absorbances of isomolar solutions of a mixture of  $\text{HMR}$  and  $\text{MR}^-$ , a solution of  $\text{HMR}$  and a solution of  $\text{MR}^-$ , respectively.

Since the equilibria of eqns (1) and (3) are assumed to be overlapping, the absorbances  $A_b$  and  $A'_a$  correspond to a hypothetical solution of the monoprotinated form ( $\text{HMR}$ ) of *o*-methyl red. Consequently, a direct determination of these absorbances is impossible. In spite of this difficulty, a graphical solution for  $K_{a2}$  and  $K_{a3}$  is still possible by rearranging eqns (6) and (7) in the following forms:

$$(A - A_a) \left( \frac{a_{\text{H}^+} \cdot f_{\text{HMR}}}{f_{\text{H}_2\text{MR}^+}} \right) = K_{a2} \cdot A_b - K_{a2} \cdot A \quad (8)$$

$$A' = K_{a3}(A'_b - A') \left( \frac{f_{\text{HMR}}}{a_{\text{H}^+} \cdot f_{\text{MR}^-}} \right) + A'_a \quad (9)$$

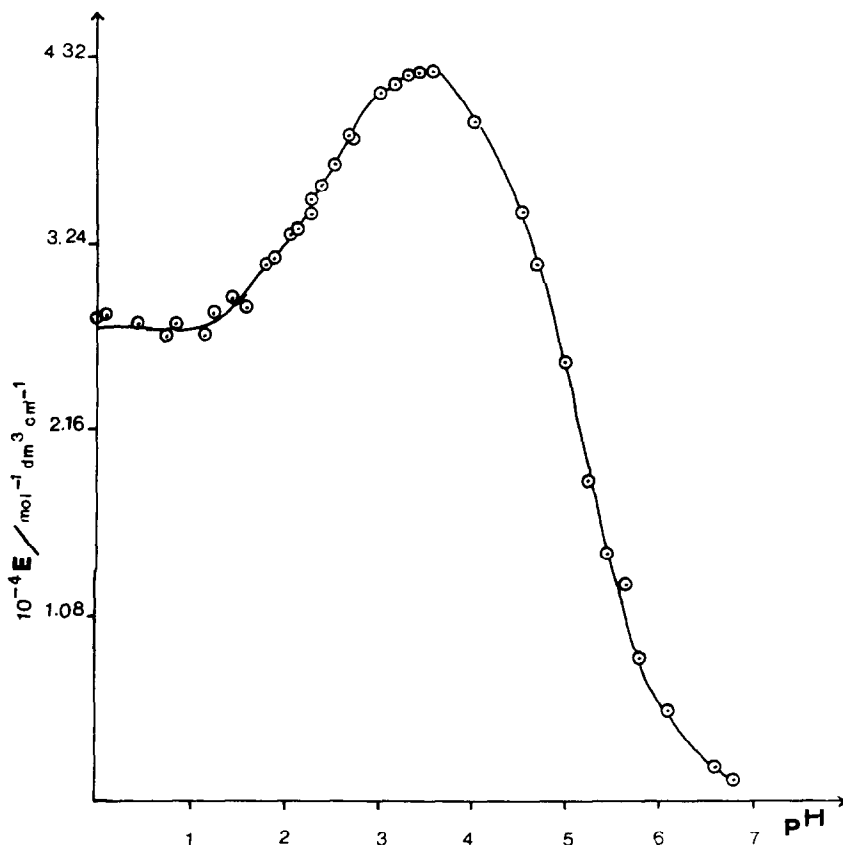


Fig. 5. The effect of pH on the molar absorptivity ( $E$ ), at 560 nm, of *o*-methyl red aqueous solution at 25°C.

Equations (8) and (9) are straight-line equations. A plot of the left-hand side of eqn (8) as ordinate versus  $A$  as abscissa should be linear with slope  $-K_{a2}$  and intercept  $K_{a2} \cdot A_b$ . Likewise, a plot of  $A'$  in eqn (9) versus  $(A'_b - A')(f_{\text{HMR}}/a_{\text{H}^+} \cdot f_{\text{MR}^-})$  should be linear, with slope  $K_{a3}$  and intercept  $A'_a$ . Ramette *et al.*<sup>6</sup> have used equations similar to eqns (8) and (9), but without considering the activity coefficients.

The equilibrium of eqn (1) becomes dominant at low pH values. We have observed that the visible spectra of *o*-methyl red recorded at low pH values (as shown in Fig. 4) exhibit a maximum difference in absorbances at 560 nm. This observation is in accord with the work of Ramette *et al.*<sup>6</sup> However, these authors have reported that the absorbance at 560 nm did not attain a constant value at low pH where the complete conversion of *o*-methyl red into the diprotic form ( $\text{H}_2\text{MR}^+$ ) is expected. Instead, it passed through a minimum and started to increase at acidities less than  $0.4 \text{ mol dm}^{-3} \text{ HCl}$ .

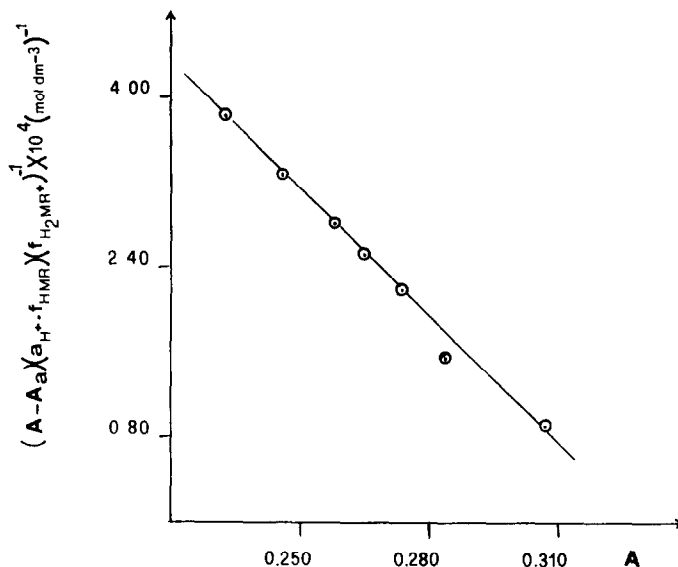


Fig. 6. Plot of eqn (8) at 560 nm. The circles represent experimental data and the line is the least-squares fit. The absorbance of the diprotonated form ( $A_a$ ) is 0.206 at pH 0.50 and  $7.43 \times 10^{-6} \text{ mol dm}^{-3}$  *o*-methyl red.

Therefore, Ramette *et al.*<sup>6</sup> have treated the absorbance of the diprotic form at 560 nm ( $A_a$  in eqn (8)) as an adjustable parameter.

We have examined the effects of pH and HCl concentration on the value of the absorbance at 560 nm of *o*-methyl red and obtained the profile shown in Fig. 5. It is evident from this figure that the molar absorptivity at 560 nm ( $\epsilon$ ) is nearly constant in the pH range 0–1. This is also true for HCl concentrations up to about  $7 \text{ mol dm}^{-3}$ . Based on these findings, we have applied eqn (8) at  $\lambda = 560 \text{ nm}$  where the absorbance of the diprotonated form,  $A_a$ , was determined at 560 nm and pH 0.5 ( $0.316 \text{ mol dm}^{-3}$  HCl), and the absorbance of the mixture at 560 nm ( $A$ ) was recorded at several pH values in the range 1.8–3.1, with ionic strength ranging from  $8 \times 10^{-4}$  to  $1.3 \times 10^{-2} \text{ mol dm}^{-3}$ .

Typical data considered for evaluating  $K_{a2}$  are plotted in Fig. 6, according to eqn (8). The values of  $K_{a2}$  were obtained by a linear least-squares method, which gave correlation coefficients of  $-0.99$  or better. Four sets of data (each set contained seven data points) were used in finding a value for  $K_{a2}$  as suggested by eqn (8). The average value of  $K_{a2}$  in water at  $25^\circ\text{C}$  was calculated to be  $(4.16 \pm 0.14) \times 10^{-3} \text{ mol dm}^{-3}$ , with a  $\text{p}K_{a2}$  value of  $2.38 \pm 0.02$ . The value reported by Ramette *et al.*<sup>6</sup> is  $K_{a2} = 4.0 \times 10^{-3} \text{ mol dm}^{-3}$ . Other older literature values of  $\text{p}K_{a2}$  were cited by Williams.<sup>5</sup> However, such literature values were obtained in ethanol–water solutions and were not specified as thermodynamic constants.

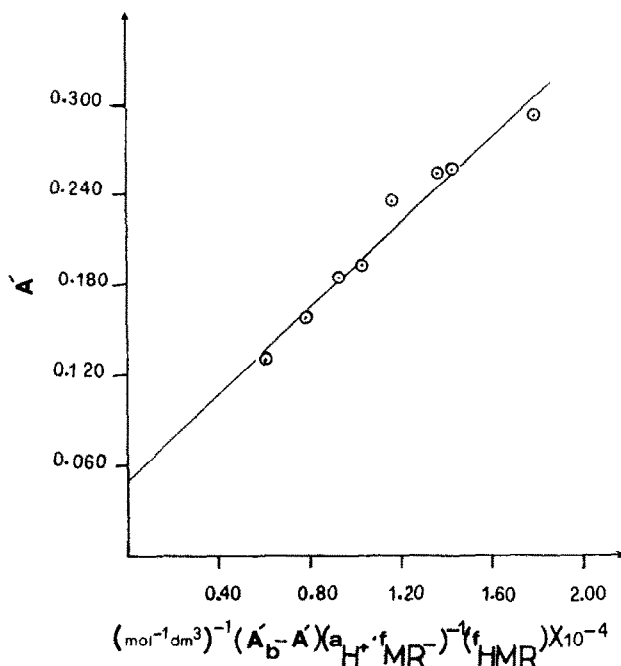


Fig. 7. Plot of eqn (9) at 400 nm. The circles represent experimental data and the line is the least-squares fit. The absorbance of the anion form, ( $A'_b$ ) is 0.351 at pH 10 and  $1.86 \times 10^{-5}$  mol  $\text{dm}^{-3}$  *o*-methyl red.

The evaluation of  $K_{a3}$  from eqn (9) was based on measuring the absorbances of *o*-methyl red solutions ( $A'$ ) at 390, 400, 415 and 430 nm in the pH range 4.4–5.5, with ionic strength in the range  $3 \times 10^{-6}$ – $4 \times 10^{-5}$  mol  $\text{dm}^{-3}$ . The absorbance of the anion form ( $A'_b$ ) was measured at pH 10. Typical data considered for evaluating  $K_{a3}$  are plotted in Fig. 7 at  $\lambda = 400$  nm. The values of  $K_{a3}$  were obtained by a linear least-squares method which gave correlation coefficients of 0.98 or better. The values of  $K_{a3}$  obtained from data at 390, 400, 415 or 430 nm for a given run were within  $\pm 2\%$  deviation from the mean value of a run. The average value of  $K_{a3}$  as obtained in this study in water at  $25^\circ\text{C}$  is  $(1.40 \pm 0.02) \times 10^{-5}$  mol  $\text{dm}^{-3}$ , with a  $\text{p}K_{a3}$  value of  $4.85 \pm 0.01$ . The value of  $K_{a3}$  reported by Ramette *et al.*<sup>6</sup> is  $1.50 \times 10^{-5}$  mol  $\text{dm}^{-3}$ . The uncertainties associated with our results represent standard deviations.

The ratio  $K_{a2}/K_{a3}$  as calculated from our results is 297, and seems to be consistent with the assumption that the two equilibria given in eqns (1) and (3) are overlapping equilibria. The simple approach<sup>1–4</sup> of finding  $K_{a3}$  from eqn (7) (activity coefficients being omitted), which relies on representing the absorbance  $A'_a$  of eqn (7) by the measured absorbance of *o*-methyl red at pH 2, is inaccurate, since *o*-methyl red cannot be completely converted into the

monoprotonated form at any pH. The profile of Fig. 5 indicates that the maximum abundance of the monoprotonated form occurs near pH 3.5. By using our results for  $K_{a2}$  and  $K_{a3}$ , we have calculated the maximum fraction of the monoprotonated form to be 0.90 at pH 3.5.

### ACKNOWLEDGEMENT

This work was supported by Yarmouk University (Project 75/84).

### REFERENCES

1. Tobey, S. W., *J. Chem. Educ.*, **35** (1958) 514.
2. Vogel, A. I., *A Text-Book of Quantitative Inorganic Analysis*, 3rd edn. Longman, London 1961, 814 pp.
3. Daniels, F., Williams, J. W., Bender, P., Alberty, R. A., Cornwell, C. D. & Harriman, J. E., *Experimental Physical Chemistry*, 7th edn. McGraw-Hill, New York, 1970, 113 pp.
4. Svec, H. J. & Peterson, N. C., *Physical Chemistry Experiments*. Iowa State University, Ames, 1978, 209 pp.
5. Williams, I. W., *Sch. Sci. Rev.*, **49** (1968) 410.
6. Ramette, R. W., Dartz, E. A. & Kelly, P. W., *J. Phys. Chem.*, **66** (1962) 527.
7. Sawicki, E., *J. Org. Chem.*, **21** (1956) 605.
8. Sawicki, E., *J. Org. Chem.*, **22** (1957) 365.
9. Sawicki, E., *J. Org. Chem.*, **22** (1957) 621.
10. Yeh, S. J. & Jaffe, H. H., *J. Am. Chem. Soc.*, **81** (1959) 3283.
11. Albert, A. & Serjeant, E. P., *The Determination of Ionization Constants*. Chapman and Hall, London, 1984, p. 17.
12. Abu-Shamleh, H. M., MSc Thesis, Yarmouk University, Irbid, Jordan, 1990.
13. Williams, I. W., *Sch. Sci. Rev.*, **49** (1968) 787.
14. Tawarah, K. M. & Abu-Shamleh, H. M., A spectrophotometric study of the tautomeric and acid-base equilibria of methyl orange and methyl yellow. *Dyes and Pigments* (submitted).
15. Rochester, C. H., *Acidity Functions*, ed. A. T. Blomquist, Academic Press, London, 1970, p. 7.